## EE 449 Milestone 5



## **Thermal Camera Team**

### **Table of Contents**

EE 449 Milestone 5	1
Executive Summary	3
Design Criteria	4
Mechanical Engineering Side	4
Thermal Modeling	10
Hardware, Electronics, Software design	20
Rotational System	22
Camera Holder	23
Leg placement	24
Controller Design	26
Bayesian Filter Theory	26
Simulations	27
Hardware	28
Power/Motor Driving Subsystem	
Optics Development and Selection	29
Electronics	
Software Designs	31
Future Work	31
Conclusion	32
References	33

## **Executive Summary**

A growing global concern is that of climate change. A major player in today's global warming problem is the greenhouse gases emitted and environmental effects of wildfires. Of special interest are those of North America where many of the ecosystems depend on fire for their sustainability. Additionally Wildfires are also increasing throughout the United States, Canada, and Mexico. For these reasons, wildfires are monitored by scientist and their impact on climate change is evaluated.

Solutions to this growing problem requires the incorporation of modern science and technology to develop novel strategies and tools to improve reduction strategies of environmental effects. An example of technological advances is the use of heat sensing devices to monitor fires at the combustion level through global scales. To monitor wildfires scientist use cameras to record the fire as it propagates and after the flames have passed. Due to the extreme heat, the cameras are under the cameras are placed in thermal boxes. However the inaccessibility to the thermal box during extreme temperatures, creates problems that lead to a loss of valuable information. To solve these challenges, this investigation proposed the development of a closed-looped thermal controlled autonomous camera housing.

Current methods of recording wildfires contain flaws due to the difficulty of observing the transition from the flaming front to the post flames due to safety and lack of mobility faced by the team conducting wildfire research. One reason for this is the cameras must be setup and left continuously running before the fire reaches the location, this is because of safety reasons for the team monitoring the fire. However, this leads to three main problems. One is battery drain issues as the camera may run out of stored power before the fire reaches there location and thus leads to information loss. The second challenge relates to storage memory because of the uncertainty of when the fire may reach the camera's location, therefore wasting valuable memory space that may be needed to record the post-flame stage combustion. Lastly, as the fire moves past the camera, the camera is limited to the direction that it was originally facing and changing the orientation manually presents a serious danger. The autonomous thermal camera housing initially proposed would be able to solve these problems using the following methods. The camera will be able to power on automatically using infrared sensors when high heat is sensed, thus conserving battery life and storage memory by keeping the camera off when it is not near the fire. Additionally the infrared sensors will be used to control the orientation the camera using the closed loop control system will point, thus facing the dace of the fire as the fire approaches. Having these features the autonomous thermal camera has the potential for profitability, as an autonomous control would increase safety for wildfire investigators, while also increasing the value of data collected.

The current status of the proposed thermal autonomous housing is of the first prototype version. This version includes an implemented PD control system, rotational system and electrical system. Additionally, the inner box of the final design was developed. The prototype was also developed to test the control system and identify areas of difficulty in the future final design. Lastly, thermal modeling was done and all parts

needed to build the final design were identified.

## **Design Criteria**

Through the development of this project our design criteria has changed dramatically but our project goal has remained the same. The primary goal of our project was to create a fully rotating camera housing that could orient an infrared camera toward an incoming fire, our current design goals are as follow:

- Withstand 1200 degree Celsius Heat for 2 minutes while exposed to direct flame.
- Withstand 300 degree smoldering temperature for 3 hours immediately after being exposed to direct flame.
- Withstand wind speeds of 50MPH.
- Keep the thermal camera under 50 degrees Celsius for the entire duration that it is out in the woods.
- Be able to conserve battery power when a fire is not present.
- Be able to rotate 360 degrees.
- Acquire the target flame in under 20 seconds (re-adjust camera position).
- Capture infrared data during the entire burning process of a wildfire.
- The setup must be light weight such that two men can hike with it. Roughly 50 lbs.
- Setup must be reusable.
- Camera must take data at 4 4.5 ft off of the ground

Our costumer Dr. Ernesto Alvarado provided these design criteria's as the camera housing will be used in different environments and types of fires. Previous work on this housing for forest fire camera turned out to be very difficult to find as the designer of the camera housing currently used has retired and no documentation was left behind.

## Mechanical Engineering Side

### System Model, System Diagram

The figure below shows a general model of the mechanical system to be controlled. This figure is highly generic but will model the behavior of our system since we also have a rotational system where the input voltage to the motor controls the motor position of an inertial mass or load. The difference between the figure below and our system is that the motor is a part of the spinning inertial mass revolving around a stationary object. The

revolving mass will be the heat shield for the thermal imaging camera and the stationary object will be the stand that elevates the camera to the desired height, optimum for data collection. the heat shield portion will contain all of the sensitive materials: thermal imaging camera, motor, microcontroller, battery and pulley system.

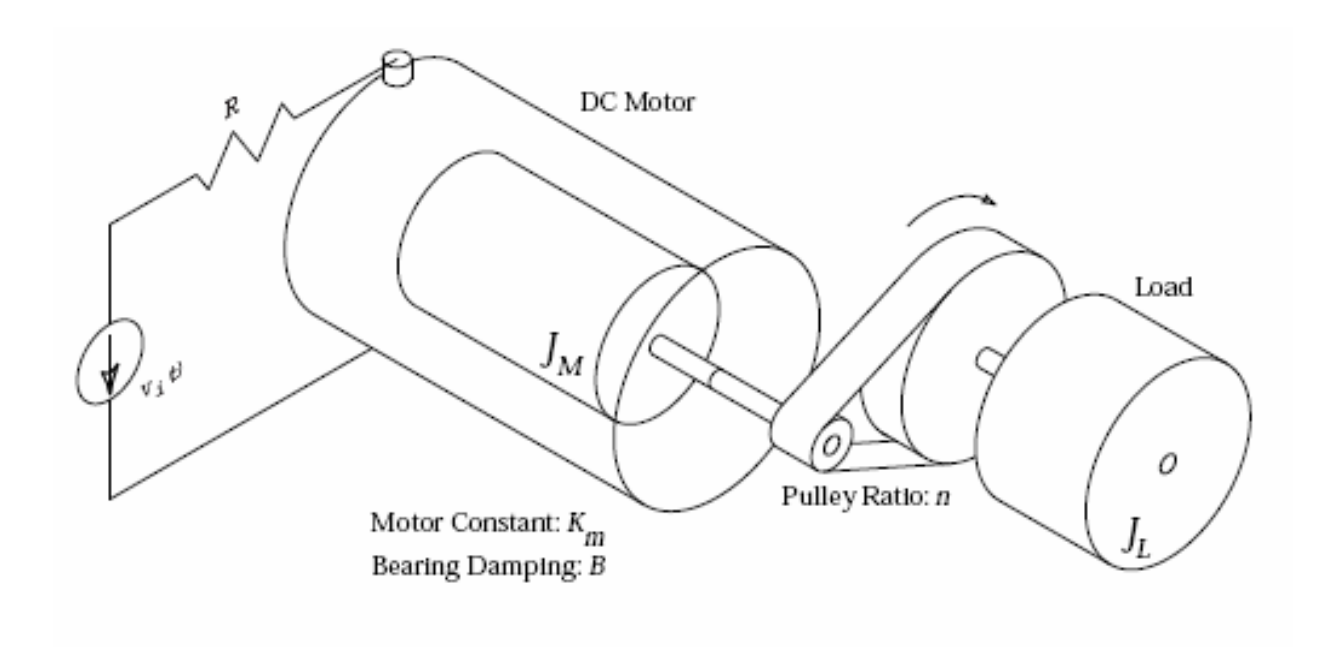


Figure: System Diagram (The controller controls the input voltage to the motor in order to control the position of the inertial load JL. The position of the motor is sent to the controller by a quadrature encoder built into the motor.

The system model was determined for the motor and inertial mass through a linear graph approach. The figure below shows the linear graph.

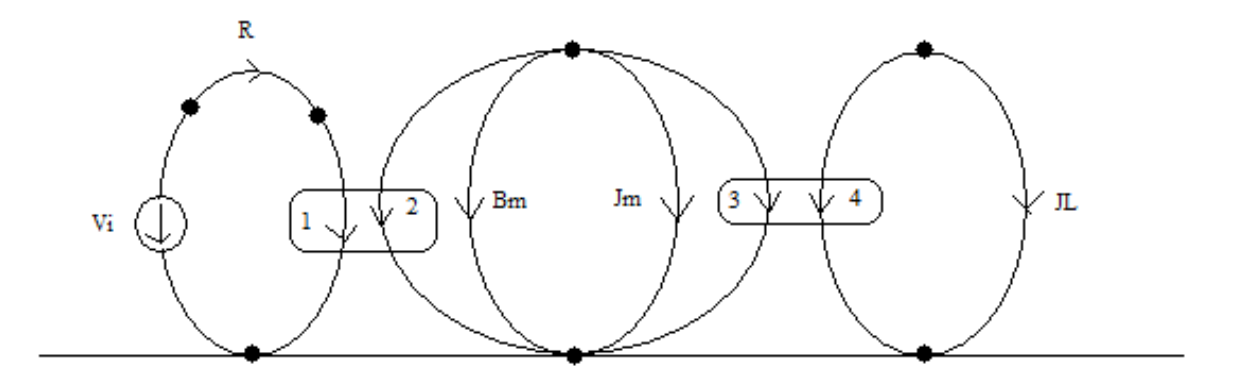


Figure: linear graph of the motor/rotational load system.

The linear graph approach can turn a complex physical system into basic circuit theory although not all systems benefit from solving for the transfer function in this way. Any rotational, translational, electrical, fluid system or any combination thereof can be broken down into mathematics resembling basic circuit theory. The line at the bottom represents the zero or equivalent of ground in an electrical circuit. Each type of system has two types of primary variables they are the across type and the through type. The across type for electrical circuits is voltage and the through type for electrical circuits is current. Since our system only has rotational and electrical systems the other primary variables for the rotational system are the angular velocity (across variable) and the torque (through variable). The ovals above represent the different types of systems involved in the math. From left to right the electrical source, the motor, the inertial load. The motor has its own inertia represented by Jm and also damping represented by Bm since the motor cannot produce a constant torque for all voltages to be realistic. Different systems can be related by transformers or gyrators. In our case we use only transformers represented by the blocks linking the ovals.

#### Process

There are three types of equations involved

- Elemental
- Continuity
- Compatibility

The linear graph can be thought of as a circuit. The continuity equations can be thought of as Kirchhoff's current law where the through variables are summed at junctions. The compatibility equations can be thought of as Kirchhoff's voltage law where the across variables around a loop all sum to 0. And the elemental equations can be thought of as basic component laws very much like the equations for capacitors, inductors and resistors that relate the two types of primary variables (Across and Through). The equations for our system can be found below.

#### Elemental Equations:

$$V_{E} = l_{E}R$$

$$V_{1} = k_{m}\Omega_{1}$$

$$T_{2} = -l_{1}k_{m}$$

$$T_{9} = B\Omega_{8}$$

$$T_{m} = \frac{d\Omega_{m}}{dt}J_{m}$$

$$\Omega_{1} = n\Omega_{1}$$

$$T_{4} = -nT_{1}$$

$$T_L = \frac{d\Omega_L}{dt} J_L$$

**Continuity Equations:** 

$$i_R = i_1$$

$$T_2 + T_B + T_{max} + T_1 = 0$$

$$T_A + T_L = 0$$

Compatibility Equations:

$$V_a = V_a + V_1$$

$$\Omega_B = \Omega_m$$

$$\Omega_z = \Omega_{m}$$

$$\Omega_{\bullet} = \Omega_{\bullet \bullet}$$

$$\Omega_{\bullet} = \Omega_{c}$$

The number of equations of each type can be found using basic linear graph rules. After obtaining these equations it takes basic manipulation to get the transfer function. Since we want to know how the motor behaves we can take the angular velocity of the motor and manipulate to get a single equation that relates the input voltage to the angular velocity of the motor ending up with our transfer function. Start with

$$\begin{split} \frac{T_{\rm en}}{J_{\rm en}} &= \frac{d\Omega_{\rm en}}{dt} \\ &\frac{d\Omega_{\rm en}}{dt} = \frac{1}{J_{\rm en}} \left( -T_{\rm e} - T_{\rm e} - T_{\rm s} \right) \\ &\frac{d\Omega_{\rm en}}{dt} = \frac{1}{J_{\rm en}} \left[ \left( \frac{k_{\rm en}V_{\rm e} - k_{\rm en}^{-1}\Omega_{\rm en}}{R} \right) - B\Omega_{\rm en} - \frac{J_L}{\pi^{-1}} \frac{d\Omega_{\rm en}}{dt} \right] \end{split}$$

$$\frac{d\Omega_{m}}{dt} = \frac{-\pi^{2}(k_{m}^{2} + k_{m}R)}{R(l_{L} + \pi^{2}l_{m})}\Omega_{m}(k) + \frac{n^{2}k_{m}}{R(l_{L} + \pi^{2}l_{m})}V_{L}(k)$$

$$\frac{d\Omega_{m}}{dt} + \frac{n^{2}(k_{m}^{2} + \beta_{m}R)}{R(l_{L} + n^{2}l_{m})}\Omega_{m}(t) = + \frac{n^{2}k_{m}}{R(l_{L} + n^{2}l_{m})}V_{l}(t)$$

Up until this point we used the angular velocity but it can be related to the position of the motor using

$$\Omega_{-} = \frac{d\theta_{-}}{dt}$$

$$\theta_{m}(t)\left(s^{2} + \frac{n^{2}(k_{m}^{2} + \beta_{m}R)}{RQ_{L} + n^{2}I_{m}}s\right) = \frac{n^{2}k_{m}}{RQ_{L} + n^{2}I_{m}}V_{L}(t)$$

Final plant model relating motor position to voltage into the motor

$$G(s) = \frac{\theta_{m}(t)}{V_{i}(t)} = \frac{\left(\frac{n^{2}k_{m}}{\mathbb{R}(J_{k} + n^{2}J_{m})}\right)}{\left(s^{2} + \frac{n^{2}(k_{m}^{2} + B_{m}R)}{R(J_{k} + n^{2}J_{m})}s\right)}$$

Final plant model relating load position to voltage into the motor

(Must be calibrated to sensors and the inertial loads must be found once the prototype is built)

Transfer function between the input motor Voltage to the position of the box

$$G(s) = \frac{\theta_{L}(t)}{V_{l}(t)} = \frac{n^{2} \frac{k_{m}}{R(J_{L} + n^{2} J_{m})}}{\left(s^{2} + \frac{n^{2} \left(k_{m}^{2} + B_{m}R\right)}{R(J_{L} + n^{2} J_{m})}s\right)}$$

#### Variables:

- Source Voltage (Input voltage to the system)
- Voltage across the resistor
- Voltage across the transformer (equivalent to the voltage into the motor)
- Angular velocity of the bearing in the motor
- Angular velocity of the motor
- $\Omega_z$  Angular velocity of the transformer into the motor equivalent to the motor angular velocity
- Angular velocity of the transformer out of the motor equivalent to the motor angular velocity
- Angular velocity transformer into the inertial mass (rotating load)
- Angular velocity transformer of the inertial mass (rotating load)
- Current through the resistor
- Current into the transformer
- Torque out of transformer from applied current
- Torque from the motor damper relative to angular velocity of the motor
- Torque on motor inertial mass
- Torque into transformer (torque from motor into gear system)

**T**<sub>4</sub> Torque received by transformer gear into the inertial mass.

**TL** Torque on the inertial load relative to the velocity

n Gear Ratio (transmits torque based on the ratio of the gears between two rotational systems)

Motor Constant (relates the input current to the motor to torque out of the motor)

#### Performance Specifications, Controller Design, Simulations

#### Old design criteria:

- Withstand 1200 degree Celsius Heat for 2 minutes while exposed to direct flame.
- Withstand 300 degree smoldering temperature for 2 days immediately after being exposed to direct flame.
- Withstand wind speeds of 50MPH.
- Keep the thermal camera under 50 degrees Celsius for the entire duration that it is out in the woods.
- Be able to conserve battery power when a fire is not present.
- Be able to rotate 360 degrees.
- Acquire the target flame in under 20 seconds (re-adjust camera position).
- Capture infrared data during the entire burning process of a wildfire.
- The setup must be light weight such that two men can hike with it. Roughly 50 lbs.
- Setup must be reusable.

#### New design Criteria

- Withstand 1200 degree Celsius Heat for 2 minutes while exposed to direct flame.
- Withstand 300 degree smoldering temperature for 2 hours immediately after being exposed to direct flame. This temperature goes down from 300 degrees C to 100 degrees C over the two hour duration.
- Withstand wind speeds of 50MPH.
- Keep the thermal camera under 50 degrees Celsius for the entire direct flame burn and smoldering
- Be able to conserve battery power when a fire is not present.
- Be able to rotate 360 degrees.
- Acquire the target flame in under 20 seconds (re-adjust camera position).
- Capture infrared data during the entire burning process of a wildfire.
- The setup must be light weight such that two men can hike with it. Roughly 50 lbs.
- Setup must be reusable.

The only design criteria that has changed since the beginning of the project is the duration and temperature of the smoldering period. The camera also only needs to take about 2 hours of video footage during the direct flame and smoldering period.

New data has been received to better understand the worst case scenario we are using as our design constraints.

Since it is no longer necessary to keep the camera under 50 degrees Celsius for 2 days while the outside is 300 degrees Celsius the simulated inside temperatures are substantially lower. The simulated internal temperatures are low enough that phase change material doesn't need to be used in order to keep the camera temperature at 50 degrees Celsius. However, due to the fact that the results come from simulation it is imperative that the device be tested to verify the results of the simulation. Initially another marketed simulation called Comsol was going to be used for validation of our heat transfer simulator. Comsol is a finite element analysis program that breaks the model up into small pieces and does an analysis on each piece individually then sums the results. During the research process it was found that the best heat transfer models in 3 dimensional simulation programs weren't all that good in the sense that all of the programs broke each 3D model up into 3 one dimensional heat transfer analysis then put them all back together for a final result. This is not true 3 dimensional heat transfer but it is the best that is on the market.

The figure below shows the worst case data provided by the customer. The black represents the temperature that the outside of the box will be exposed to.

## **Thermal Modeling**

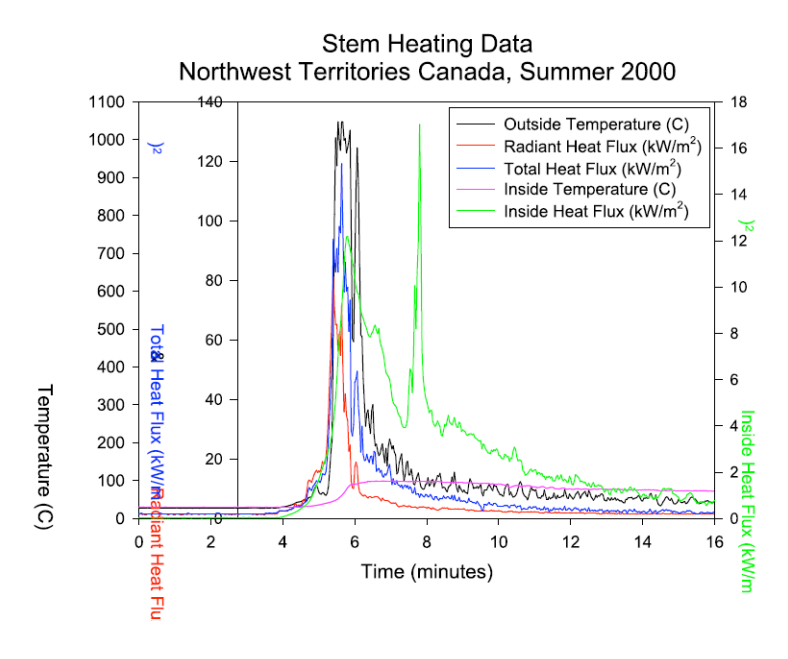


Figure: Recent addition to the temperature data recovered from wildfires

The control used to keep the temperature down is open loop control. This is made up of two parts. Those parts are the insulation and the phase change material. The simulations that would incorporate the phase change material haven't yet been completed due to time constraints. However, with the new design criteria the simulations show results that would not need phase change material. Although this is not an excuse to not include the phase change material. These results can be seen below.

#### Simulations

The finished Comsol model can be seen below.

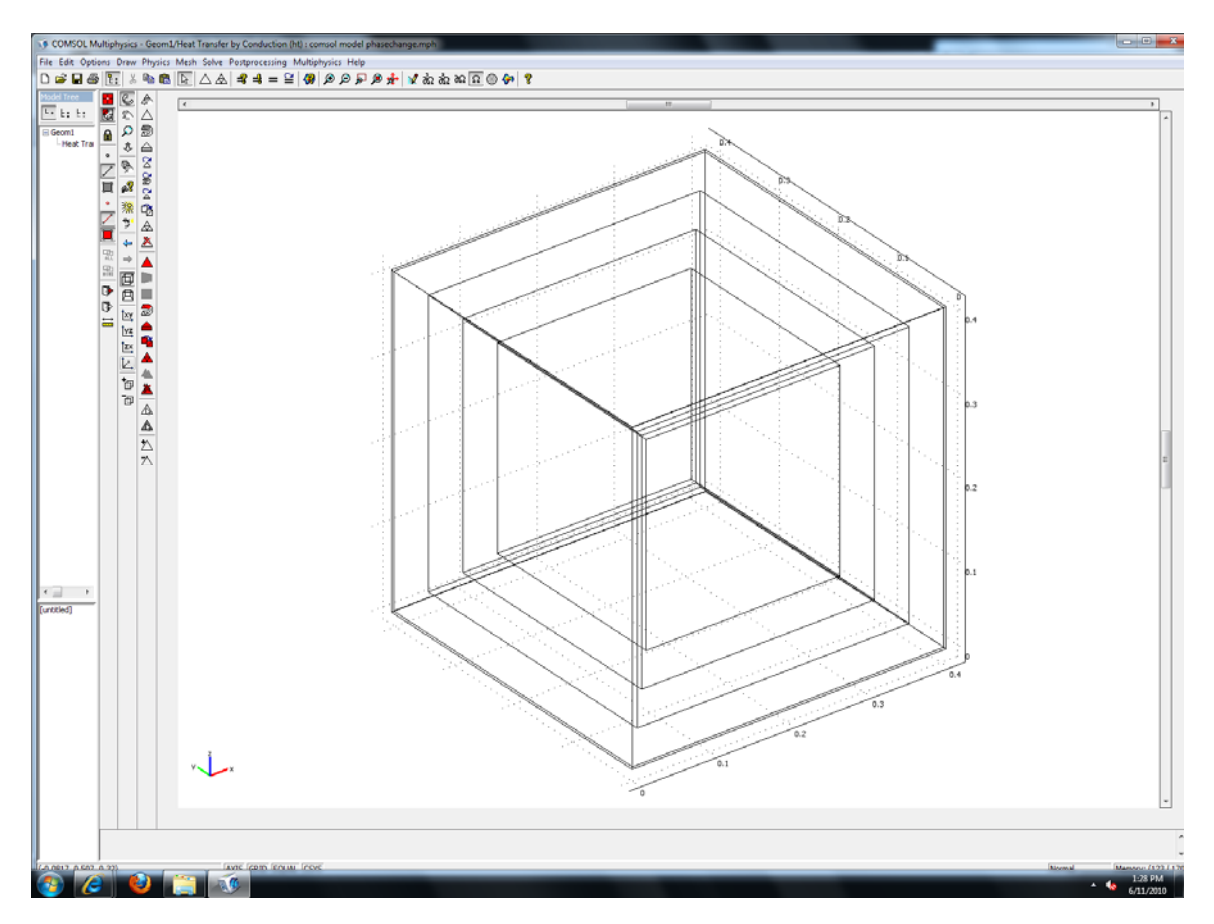


Figure: Comsol model of the box with insulation(1" firebrick and 1" pyrogel) and 1" phase change material layers as well as the air in the middle of the box. All of these are thermal loads with their individual material properties put into the program.

The Comsol FEA model above was set to run a transient heat transfer analysis that would allow us to pick any point within the model of the box and generate a temperature distribution over time at that point. This could be done many times with different points all plotted on the same graph to compare different temperature distributions within the box. There are three problems with this model. The first is that the boundary conditions

of a changing external box temperature can be added but haven't worked on less complex models. Also the phase change materials use this type of logic within the program in Comsol they are called Heaviside equations. The phase change material properties are also not working at this point. The last and final problem is that since this is a transient conduction 3 dimensional heat transfer model the number of elements in the mesh is over 1 million. The computing power required to run this simulation within a reasonable amount of time is beyond the ability of the typical lab computers with this software. These are the reasons our rudimentary FEA model created in Matlab hasn't been compared to a marketed heat transfer analysis program at this point.

The figure below is an example of the types of heat distribution we can achieve in a comsol model although the picture below was taken at a very short period of time after a heat source on the outside of the box was added hence the very cool inside and extremely hot outside. The internal insulations used was aerogel.

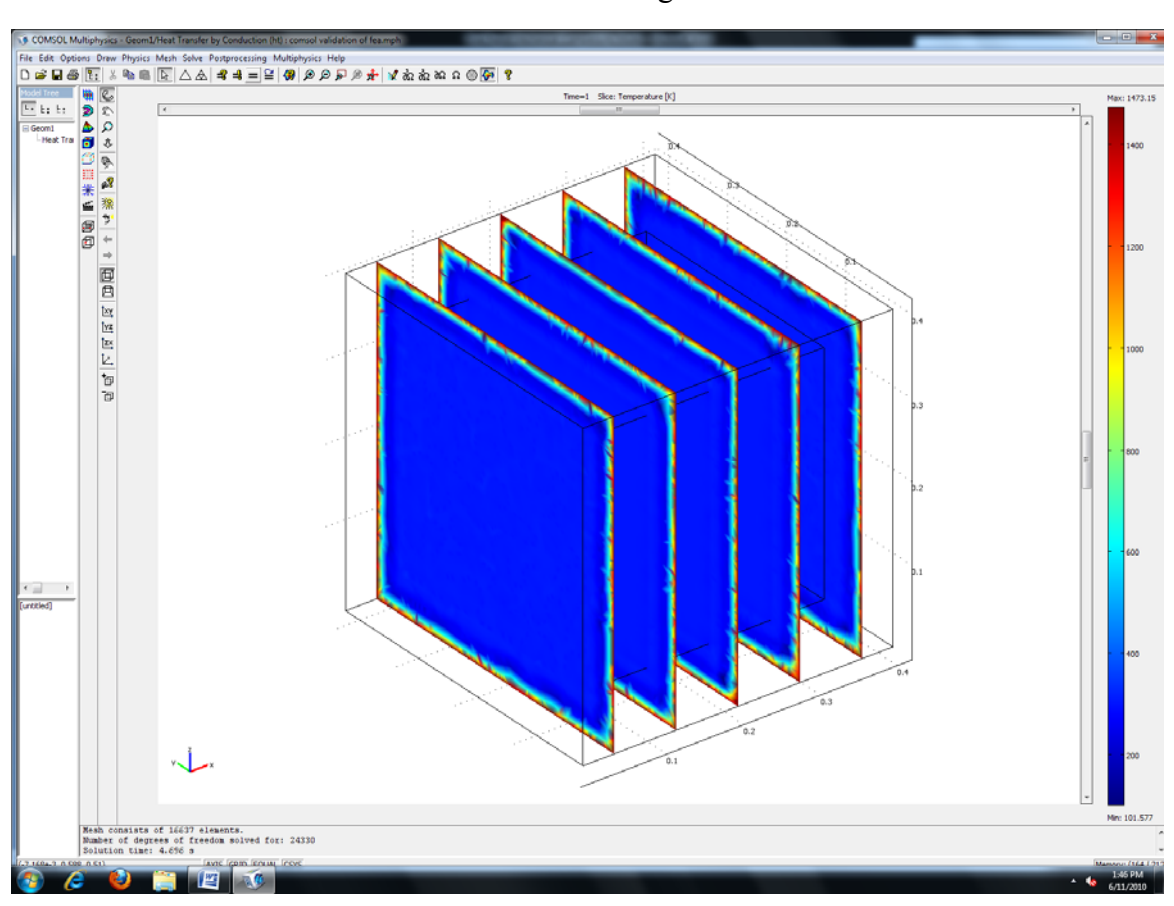


Figure :Aerogel insulation exposed to 1200 degree Celsius temperature for a couple seconds with air inside as another themal load. Since the thermal conductivity of both the air and Aerogel are so low the surface temperature is extremely hot at 1200 degrees Celsius and the inside temperature of most of the box is at a cool 27 degrees Celsius (assumed ambient temperature). The low internal temperatures are due to a small amount of exposure to a heat source.

Using the Matlab FEA created for this project this simulations below show the results of the insulations we have tested in theory.

Test of typical firebrick

6 minutes at 1200 C (over engineered version)

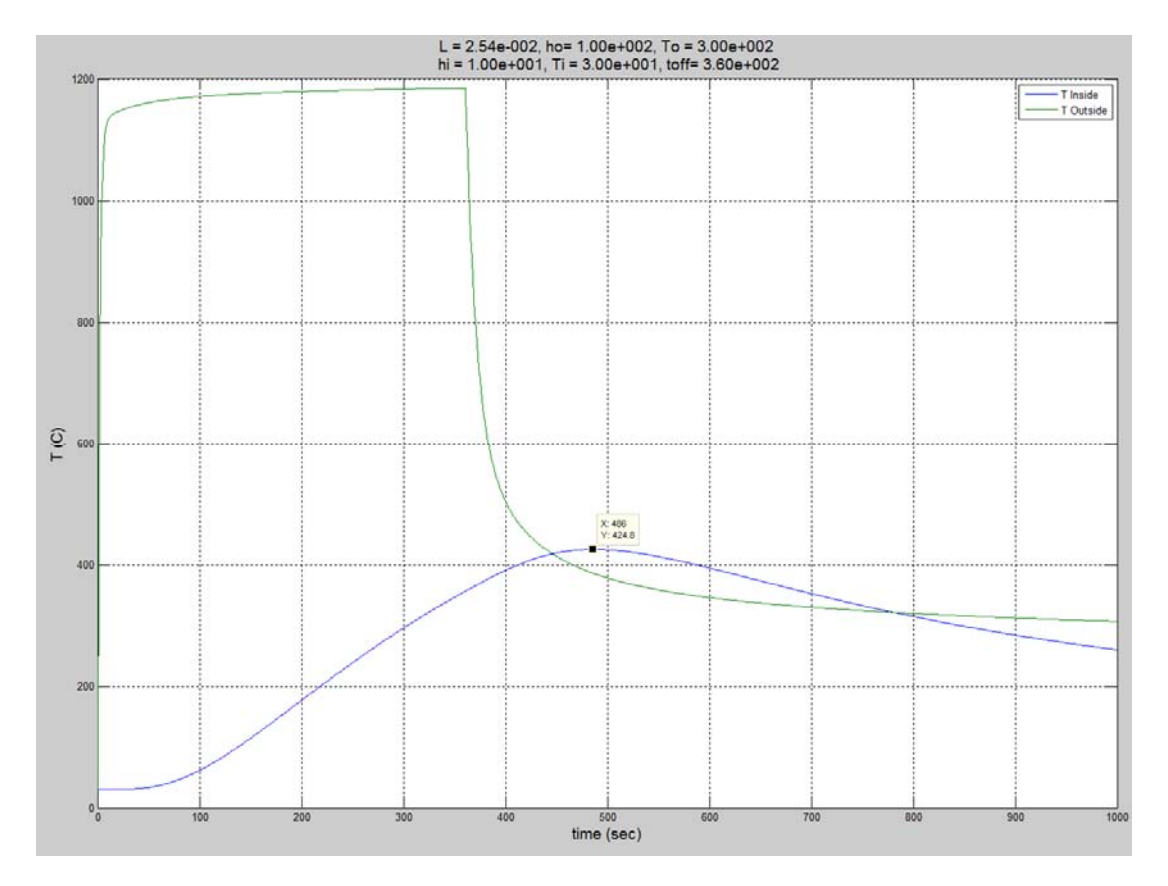


Figure: 1 inch firebrick exposed to 1200 degree flames for 6 minutes hits a maximum temperature of 424.8 degrees Celsius on inner surface. The steady state temperature is 172.6 degrees Celsius for 1 inch firebrick under the 6 minute condition.

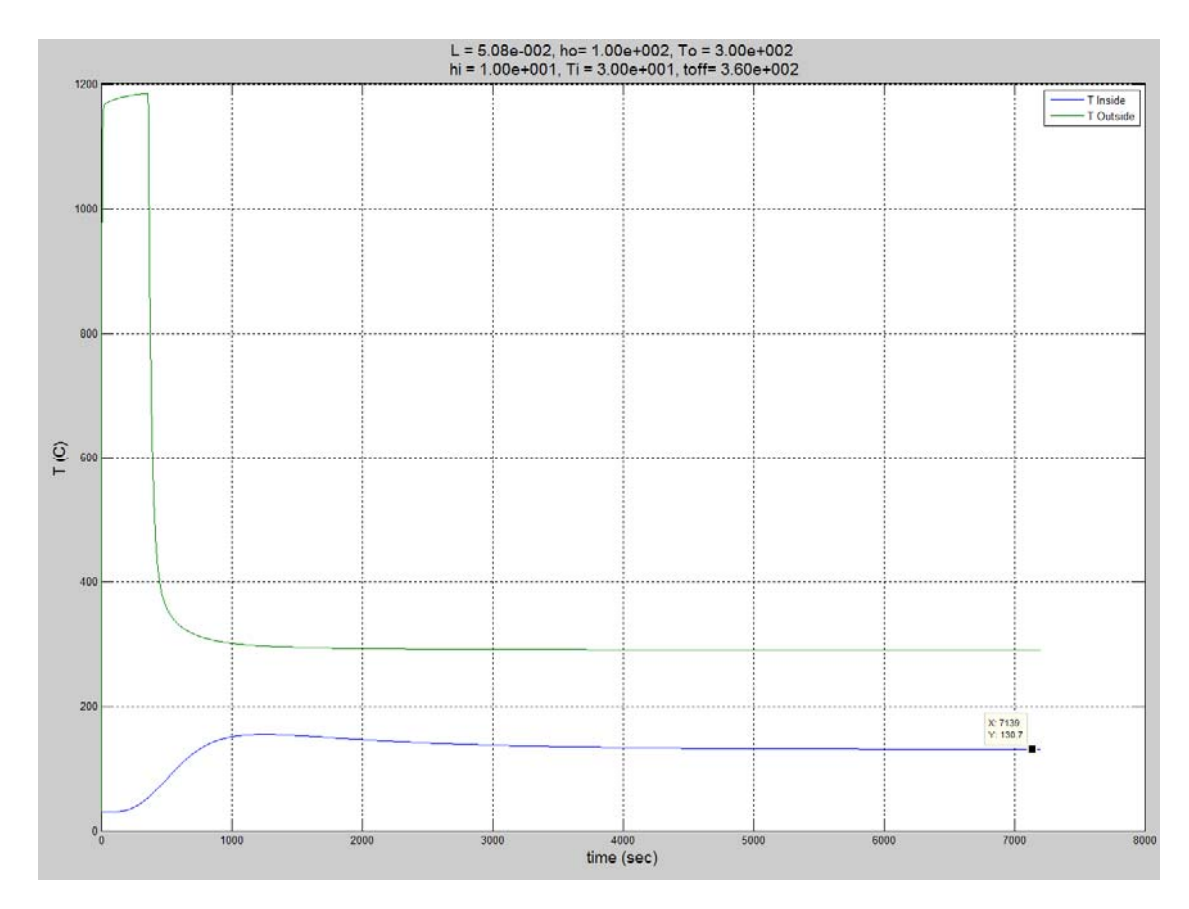


Figure: 2 inch firebrick exposed to 1200 degree flames for 6 minutes hits a steady state temperature of 130.7 degrees Celsius on inner surface. With increased thickness the maximum temperature on the inner surface of the fire brick is 154.3 degrees Celsius much less than the 424.8 degrees Celsius inner surface temperature of the 1 inch thick firebrick under the same conditions.

The above conditions were original attempts to add some extra protection against the uncertainty of the wide range of conditions the box would face in a harsh environment. After receiving the new design criteria with the knowledge that the data received along with it was the worst case scenario the amount of over engineering was reduced.

2 minutes at 1200 C (meeting the design criteria)

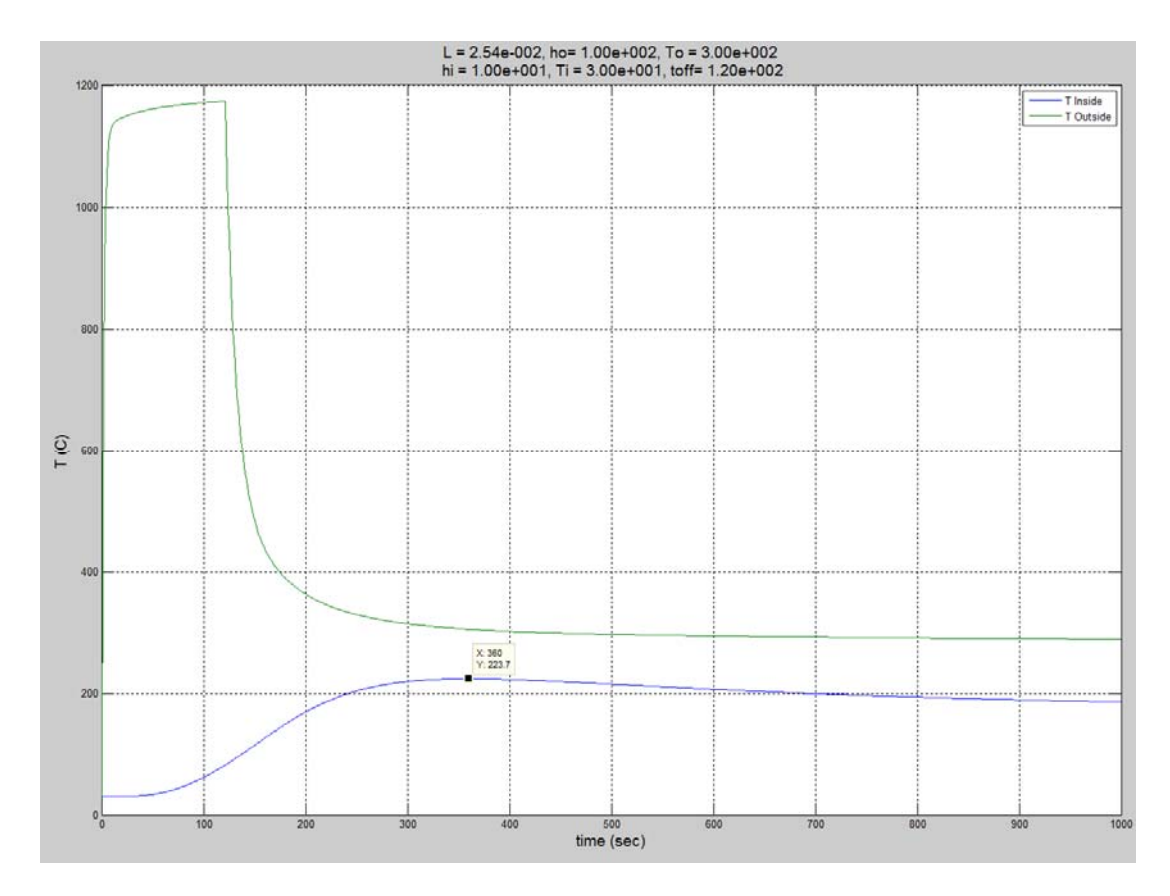


Figure : 1 inch firebrick exposed to 1200 degree flames for 2 minutes hits a maximum temperature of 223.7 degrees Celsius on inner surface. The steady state temperature of 1 inch fire brick is 172.6 degrees Celsius under the 2 minute condition.

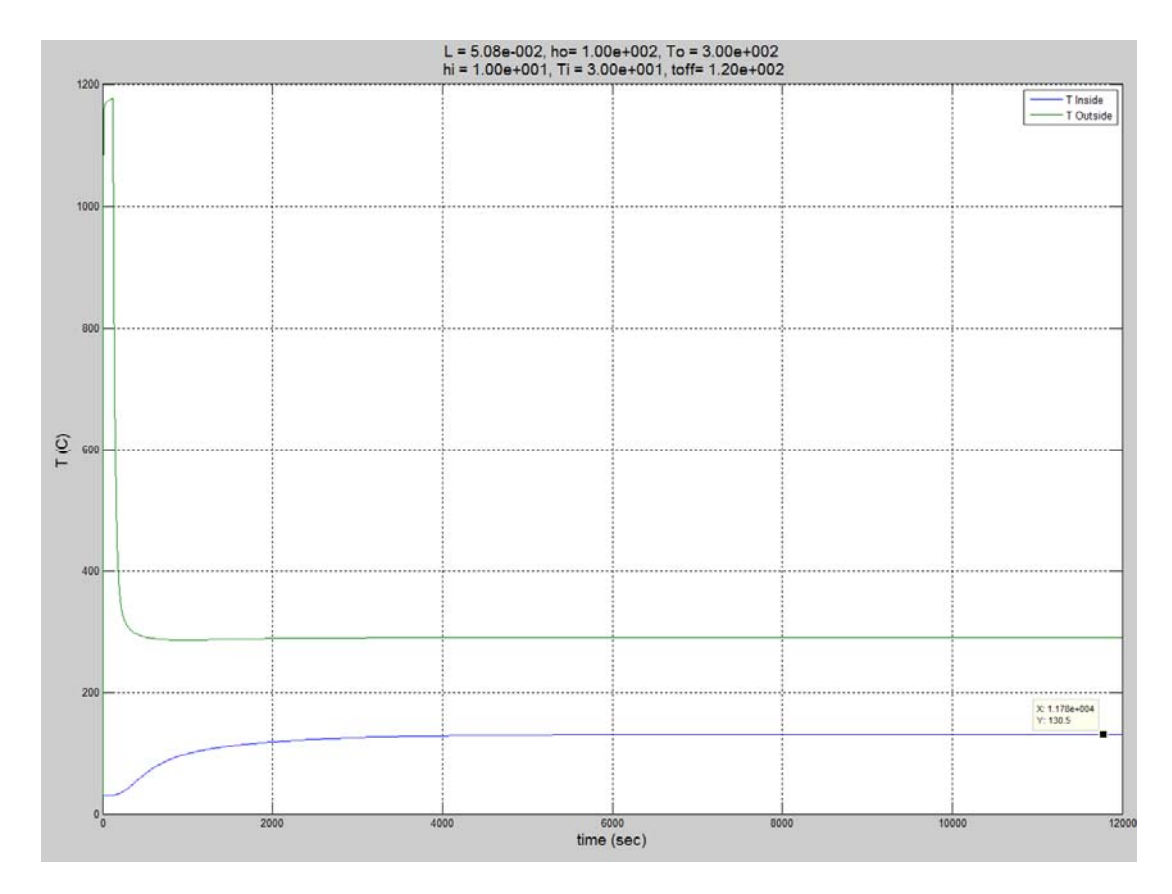


Figure: 2 inch firebrick exposed to 1200 degree flames for 2 minutes hits a steady state temperature of 130.5 degrees Celsius on inner surface. With increased thickness the maximum temperature on the inner surface of the fire brick is also 130.5 degrees Celsius much less than the 223.7 degrees Celsius inner surface temperature of the 1 inch thick firebrick under the same conditions.

From the previous 2 graphs it can be seen that even though the firebrick can block the heat flow extremely well at very high temperatures eventually the inside surface of firebrick will reach temperatures above our design criteria before the 2 hour smoldering period is up making its use alone unacceptable.

Test of Pyrogel

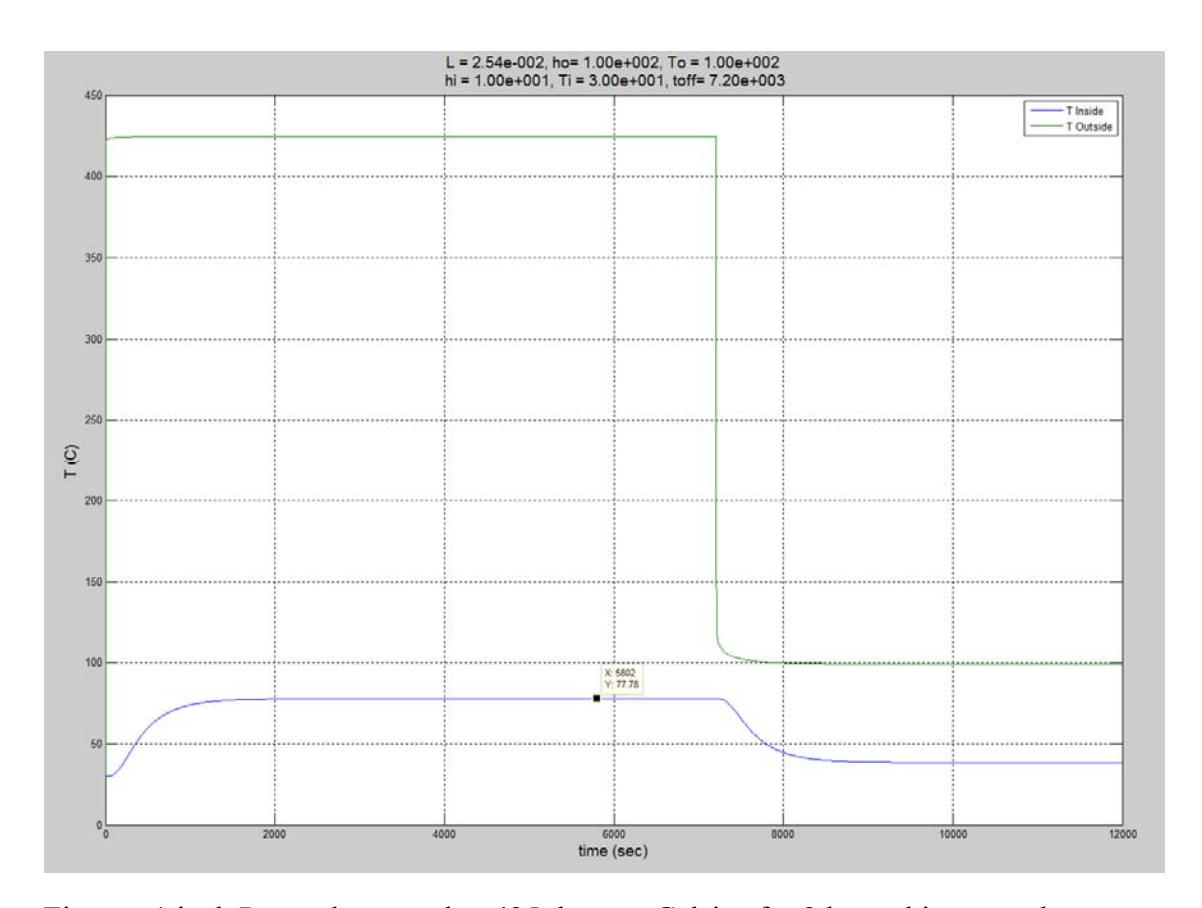


Figure: 1 inch Pyrogel exposed to 425 degrees Celsius for 2 hours hits a steady state temperature of 38.38 degrees Celsius. It hits a maximum temperature of 77.78 degrees Celsius for about 8000 seconds.

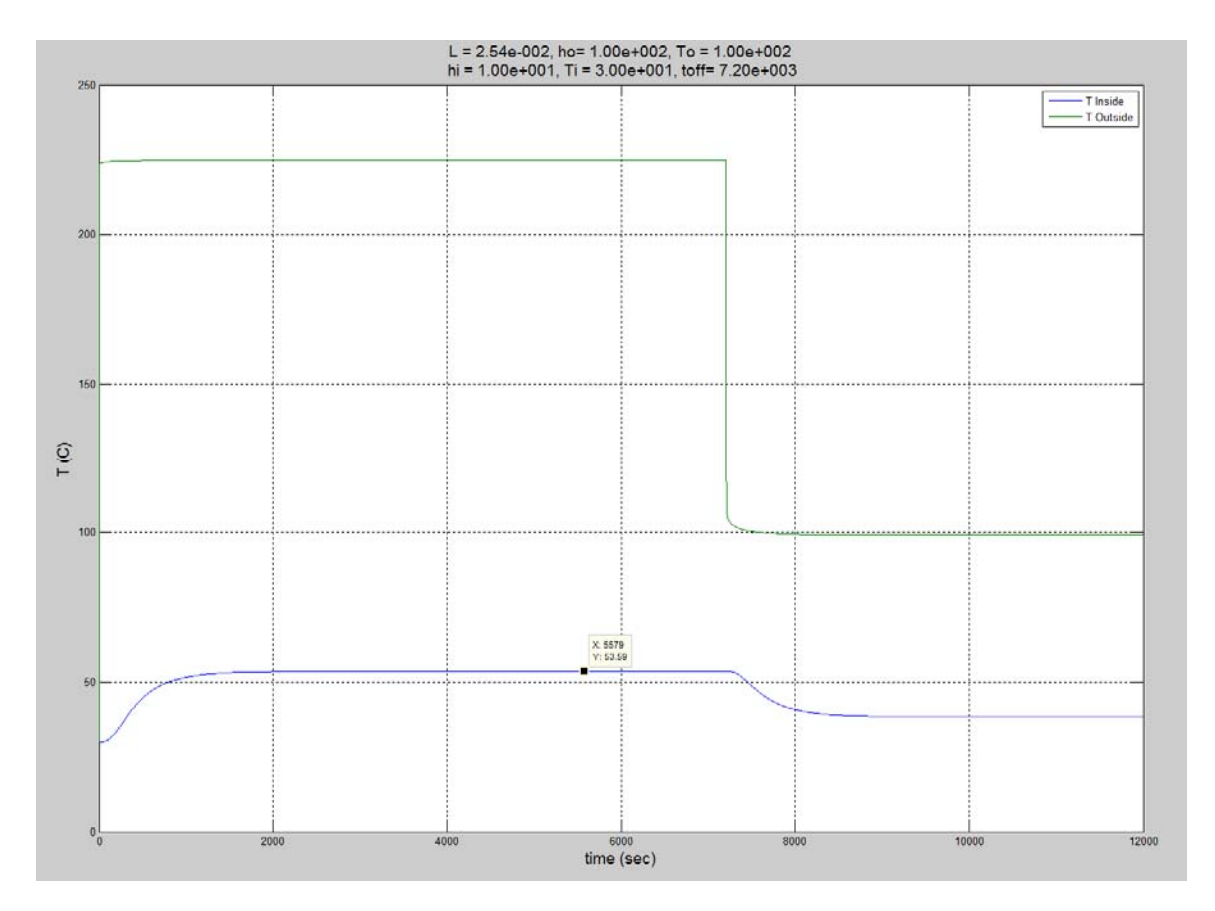


Figure: 1 inch Pyrogel exposed to 225 degrees Celsius for 2 hours hits a steady state temperature of 38.39 degrees Celsius. It hits a maximum temperature of 53.59 degrees Celsius for about 8000 seconds before dropping to 38 degrees Celsius.

Both of the simulations of the pyrogel were created with a starting temperature equal to the maximum temperature on the inside surface of the firebrick after having experienced a 1200 degree burn. It is known that the smoldering period hits 300 degrees Celsius right after being exposed to 1200 degree Celsius direct flame but drops off to 100 degrees Celsius after a two hour period. Since the rate at which the temperature drops off is variable the assumption was made that if the maximum temperature of the inside of the fire brick was constantly applied for the two hour smoldering period instead of dropping off, the internal temperature of the pyrogel would be greater than the actual value. Thus if this temperature met the design requirements the system would most definitely work in theory.

In order to optimize the insulation the use of firebrick was necessary to take the bulk of the heat initially and the pyrogel was needed to reduce the internal box temperature of the camera to at or below the performance specification of 50 degrees since it is the best insulator but cannot handle temperatures as high as the firebrick. With the use of both insulators with an inch thick of each the maximum temperature the camera would experience is 53 degrees Celsius without the inclusion of a phase change material. There are many reasons why the simulation might not match what actually happens. These include the case where the temperatures that the box experiences are either higher than

what was predicted or the durations where fire is exposed to the box last longer than originally thought as well as the material properties of the materials not matching the data sheets we used to get all of the material information.

The phase change materials will still be included as a form of failsafe incase these problems are run into in the future development of this project.

#### Principles of rudimentary Matlab FEA design

The only thing necessary to control on the mechanical side is the internal temperature of the box. Although this task is not in the scope of this course due to the fact that it is open loop control, it is still a difficult task to achieve due to the extreme temperatures we are working with and heat transfer implications. Due to the fact that the system has open loop control the end steady state result will eventually level off at an internal temperature that is dependent on the mechanical properties of the materials we are using as well as the external conditions. This end steady state result is the state at which the phase change material we are incorporating will be all used up. Thus the only thing stopping the heat from entering the box will be the insulation.

The open loop control system we are implementing to do this task requires two stages of protection from extreme heat. The two stages are the outer insulation and the phase change material. The outer layers of insulation shield the sensitive equipment inside the box by effectively reducing the cold face surface temperature by more than half the outside temperature. It is physically impossible to keep the temperature inside the box below 50 degrees Celsius by only using insulation (at least the kind affordable for students).

At this point in order to simulate the transient behavior of the temperature distribution, Matlab was used to generate a rudimentary Finite Element Analysis program with the help of professor Ashley Emery. This FEA program was able to mesh to a desired accuracy although we found that refining the mesh didn't provide much accuracy at the cost of computing time. The programs end result is a temperature vector with the current temperature at each different location throughout the plane wall. The FEA program operated based off of a single principle the law of the conservation of energy in heat transfer form. This principle was implemented at each and every finite element throughout the plane wall. The math for the A matrix looked something like this

Energy balance on Hot face

$$\frac{\rho c \Delta x}{2} \times \frac{T_1^{m+1} - T_1^m}{\Delta t} - \left(T_{co}^{outstde} - T_1\right) k_{outstde} + \frac{(T_2 - T_1)k}{\Delta x}$$

Energy balance in middle of insulation (General)

$$\frac{\rho c \Delta x}{2} \times \frac{T_1^{m+1} - T_1^m}{\Delta t} = \frac{(T_1 - T_2)k}{\Delta x} + \frac{(T_2 - T_2)k}{\Delta x}$$

There are more of these just depends on how refined the mesh is.

Energy balance on Cold face

$$\frac{\rho c \Delta x}{2} \times \frac{T_N^{m+1} - T_N^m}{\Delta t} = \left(T_{\infty}^{bookdo} - T_N\right) h_{bookdo} + \frac{(T_{N-1} - T_N)k}{\Delta x}$$

Variables:

T: temperatures of various locations inside a plane wall (degrees Celsius)

• : density of the plane wall (kg/m<sup>3</sup>)

c: specific heat of the plane wall (J/kg\*K)

t: time increments (seconds)

x: the length of an individual node in the plane wall (meters)

N: number of nodes in the plane wall (unitless)

k: coefficient of thermal conductivity (W/m\*K)

h: coefficient of thermal convection (W/M^2\*K)

The equations consider the conduction of heat through the inner elements. The equations differ when it comes to the outside elements. Namely the first and last row of the A matrix. These two parts need to incorporate the heat transfer by convection into the equation. The convection comes in on both sides of the insulation assuming a fluid layer on each side. Once the A matrix is set up an iteration technique is used to generate corresponding temperatures throughout the material at each interval in time. The increment of time for our case is 1 second.

With the FEA program up and running we can do simple calculations of transient conduction through a plane wall. However, at this stage of the program we can only consider a single type of material. In future reports we hope to have a more complete program to help us run simulations on both stages of the heat control process with two types of insulation and a phase change material included.

# Hardware, Electronics, Software design

- Solidworks and design of the stand
- Prototype and simplifications

#### Hardware

#### **Materials**

#### Titanium Alpha Beta

As of this stage in the design process this is the current best metal for the job of holding the heat shield together. It was suggested we use this type of titanium for wildfire applications by another mechanical engineer that specifically builds devices that go inside wildfires. It will be able to withstand the high temperatures required and be more easily weldable than the inconel. However, the problem with titanium is that specialized cutting tools will be required to machine any titanium parts and will also have to be purchased.

#### Firebrick

The primary insulator in this project is insulating firebrick. There are different types that are used in kilns and ovens that do heat up rather quickly to attain specific cooking temperatures. We have chosen an insulating type that will shunt the majority of the heat during the time of extreme heat exposure to the outside of the box while in direct flame. The problem is that eventually the insulating firebrick will reach temperatures well above the design criteria. It is cheap and easy to work with.

#### Pyrogel

The best insulator we are using is an off branch of aerogel. This type of aerogel is not very high temperature in the sense that it cannot handle 1200 degree temperatures due to its primary use in protective clothing. Its maximum temperature is 600 degrees celsius. It is much more dense than normal aerogel and has about the same thermal conductivity meaning it can better insulate than normal aerogel at lower temperatures.

#### Plus ice

The specific type of phase change material we are using is called plus ice X40. The name is linked to the fact that its phase change temperature is 40 degrees Celsius. This is good because unless ambient temperatures where this device will be used are above 40 degrees Celsius the plus ice will retain its energy absorbing abilities without melting like ice would in the same conditions. Plus ice x40 can be frozen and refrozen for reuse. The phase change occurs in the form of a change in crystalline structure at well defined temperatures.

	Plusice Solid-Solid PCM Solutions											
PlusiCE Model	Phase Change Temp. (*C)	Phase Change Temp. (F)	Latent Heat (kJlkg)	Latent Heat (Btuffb)	Density (g/cm3) below PCT	Density (IbIf3) below PCT	Density (g/cm3) above PCT	Density (lb/ft3) above PCT	Thermal Conductivity (Wim K) below PCT	Thermal Conductivity (Btu /f2 h F) below PCT	Thermal Conductivity (Wilm K) above PCT	Thermal Conductivity (Btu I ft2 h F) above PCT
PlusICE X40	40	104	131	56	1046	65	986	62	0.253	0.146	0.209	0.121
PlusiCE X80	80	176	192	83	1193	74	1120	70	0.361	0.209	0.335	0.194
PlusiCE X180	180	356	301	129	1330	83	1220	76	0.993	0.574	0.508	0.294

Figure: Relevant properties for calculating how much energy the plus ice can absorb

#### Stainless steel

Stainless steel will be used for the camera holder and inner box. The reason for using stainless steel is because it is cheap and easy to work with as well as its material properties to reflect the majority of radiation heat transfer coming into the box. Since the Aerogel will decrease the amount of heat energy coming into the box stainless steel will work for handling a couple hundred degree temperatures not that it will need it. The stainless steel also has good corrosion and oxidation resistance. Depending on how the hikers will divide the load the stainless steel will not corrode or oxidize under normal conditions due to its chromium oxide layer. This protective layer will regenerate if scratched off depending on the amount of damage since chromium makes up more than 10.5 % of any type of stainless steel. The chromium bonds with the oxygen in the air and reforms the layer automatically if damaged.

## **Rotational System**

The rotational system was unavoidable in meeting the design requirements and class requirements of incorporating a control system in the project. This rotational system needed some kind of gearing and an actuator attached to the controller with sensors such that the camera view could be altered to improve the consistency of data collection. This rotational system meant that the box would need to be sealed off to the outside since it would be directly exposed to flame. The initial idea was to run a peg up into the box fixed to the stand and connect the peg to the gear system allowing for motion. The problem with that idea was the sealing of the box. The insulation would need to be able to seal against the peg and thus friction would cause wear in the insulation and eventually fail quickly due to the abrasion of the insulation against the peg. The replacement was a hexagonal or other shaped billet with a wide bottom such that any holes in the bearing could be covered up on both the inside and the outside of the box. The inside would be covered by the insulation and the outside part of the exposed bearing would be covered by the extended base of the hexagonal piece.

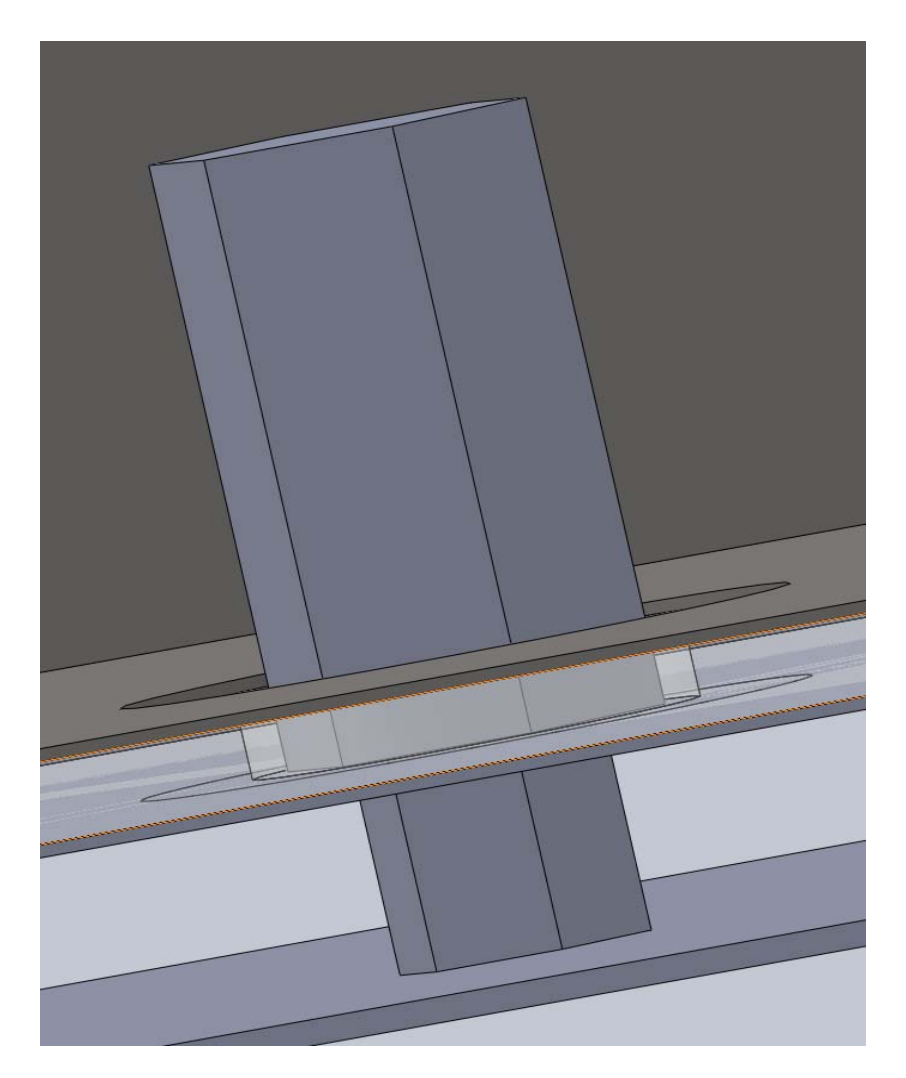


Figure: The Aerogel insulation is the transparent material between the inner stainless steel box(top) and the outer Titanium box(bottom) it is staggered with the gap between the Titanium and the bearing to seal off the inside from the fire.

## Camera Holder

The purpose of the camera holder is to isolate the camera position in the box to a level that allows the lens of the camera to align with the sapphire window to see outside. It also holds the circuitry and battery and surrounds the camera with a secondary stage of phase change material. The camera holder also has an open area as viewed from the left that allows the gear system to go underneath and connect to the female hexagonal piece to complete the rotational system. The camera holder is made of stainless steel just like the inner box that pins the Aerogel in place along the walls of the outer box. The main purpose is the isolation of the camera, the circuitry and especially the battery. The

sensitive components are kept as far from the heat source as possible. It is held in place by blocks of phase change material between the inner box and the camera holder. Figure below shows a picture of the camera holder concept.

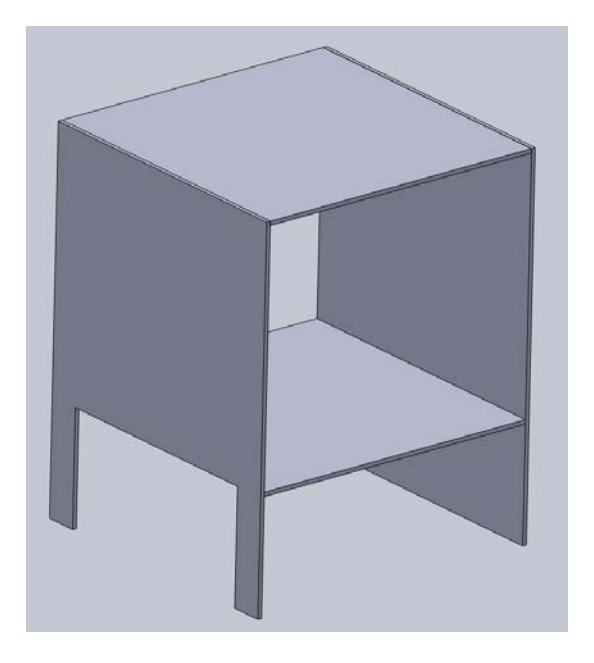


Figure: Camera holder

The size of the outer titanium alpha beta box depended solely on the size of the contents inside. Since our component dimensions are fixed the deciding factors for the final dimensions were the insulation and the phase change material. Unfortunately the size was an estimate and has not been finalized at this stage. The balance between phase change material and the insulation is the reason for this. The final amount of phase change material has not been found and thus the dimensions are at this point an educated guess.

## Leg placement

The leg placement is dictated by the size of the box that the stand supports. With the size estimated at being 16 inches per side of the cube, the amount of drag force on the box had to be determined. The Design criteria that we were given stated that the heat shield would have to withstand 50 MPH wind speeds. The drag force on simple objects can be calculated using the drag equation shown below which is valid for Reynolds numbers greater than 1000.

#### Drag Force

$$P_0 = \frac{1}{2}\rho C_0 A v^1$$

where

 $F_D = drag force (N)$ 

 $\rho$  = mass density of the fluid (kg/m<sup>3</sup>)

 $\mathbf{v}$  = velocity of the object relative to the fluid (m/s)

A = reference area perpendicular to fluid flow (m<sup>2</sup>)

 $C_D$  = drag coefficient dependent on the geometry of the object (dimensionless)

#### Reynolds Number

$$Re = \frac{\rho V L}{\mu}$$

where

Reynolds Number (dimensionless)

 $\mathbf{P} = \text{density of the fluid (kg/m}^3)$ 

V = mean fluid velocity (m/s)

L = characteristic linear dimension (travelled length of fluid) (m)

We looked at different situations and found that the properties of air change at different temperatures. The drag forces at three different conditions were tested. The conditions were the normal conditions at 27 degrees Celsius, the smoldering conditions at 300 degrees and the peak temperatures at 1200 degrees Celsius. As the temperature increased the density of air decreased and thus the drag forces also decreased. Also the orientation of the box in the fluid flow directly affects the drag forces. The assumption made was that the wind was blowing parallel to the ground. The orientation of the box that generated the highest amount of drag was when a side of the box was perpendicular to the fluid flow. This produced a drag coefficient of 1.05. The more dense the fluid the higher the drag force. This is the worst case scenario unless working with 50 MPH wind at freezing temperatures. The maximum drag force on the box at normal conditions was

$$L = 16$$
" = 0.4064m  
 $50MPH = 22.352 \text{ m/s}$ 

$$ho_{
m etr} = 1.1614 rac{kg}{m^3} m{\oplus} 300K m{\oplus} 1atm$$

$$P_0 = \frac{1.1614 \frac{kg}{m^2} \times \left(22.352 \frac{m}{s}\right)^2 \times 0.8 \times 0.165161 m^2}{2} = 38.3338 M$$

After calculating the maximum drag on the box the rest is just a simple statics problem. The weight of the box was assumed to be 30 pounds and the height of the camera lens was taken to be 4 ft. so the leg height was then 39". From this the leg positioning was calculated such that if the box were 30lbs or greater then the box will resist 50 mile per hours winds.

## **Controller Design**

The controller architecture of this project experienced significant change and iterations through the course of the design and implementation. The first design, a comparator based fire tracker utilized a simple set of conditions for centering the fire. In summary, it compared all six thermopiles and would seek such that the measured incident thermal energy at the front-facing sensor was greatest.

Due to its highly nonlinear nature, this design was abandoned in lieu of a Bayesian Filter based estimator. This estimator used probability distributions scaled by the measured values of the thermopiles added together and scaled to a constant summed value.

With this new algorithm, the topology of the system is reorganized to have the estimator reading the sensors and producing a specific target angle for the inner position loop to track to. While still an inner-outer loop design, this eliminates the linearity concerns presented by Dr Klavins and Charlie.

## **Bayesian Filter Theory**

The replacement estimator design proposed my Dr Klavins, known as "Markov Localization," is a simple form of Kalman filter described as a Baysian filter. This

estimator works by making certain assumptions on the sensors, particularly that given a particular value, there is a normally distributed probability of where the actual signal is around where the sensor is pointing.

Since a normal distribution is almost always a reasonable representation of the probability distribution of a sensors, a Gaussian was used to compute this curve. In implementation, the estimator created Gaussian distribution of the roughly arbitrary form:

$$b(\theta) = \text{sensorVal} * e^{\theta/128}$$

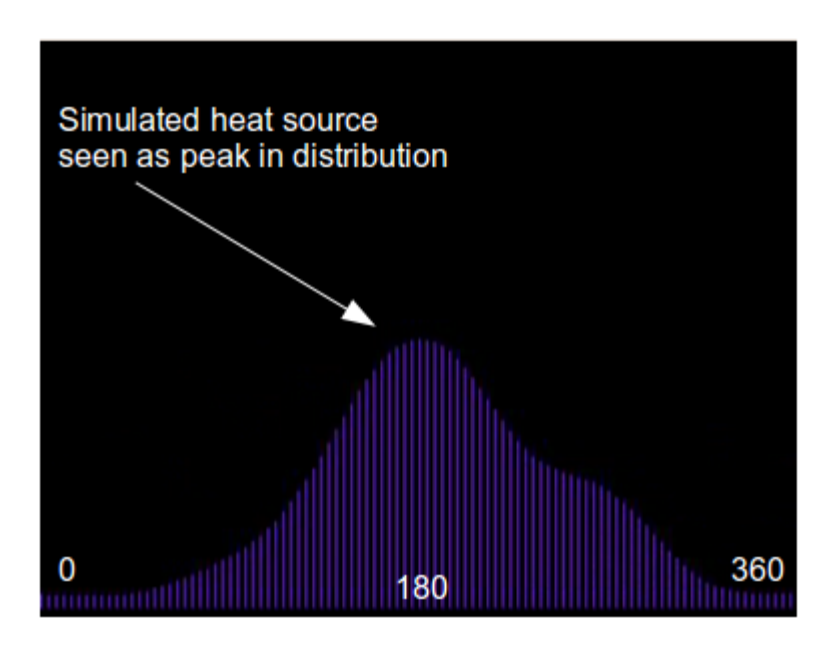
[Figure: The equation used to create a Gaussian distribution for the estimator.]

With this distribution scaled and shifted for each sensor and its respective current value, a summation of all the sensors' curves was computed. This summation curve was then scaled to standardized height and averaged with the previous sensor readings over time.

This estimator, in theory, is designed to help reduce error from noise and provide as accurate a guess as to the actual location of the fire as possible. In practice, there were several problems that likely stemmed from a lack of depth of understanding on the topic. These included a slow response to sensor perturbations as well as a failure to gracefully handle large noise signals on the sensors[Fox].

## **Simulations**

In order to test the behavior of the estimator, perturbations were applied that demonstrated what was believed to be typical behavior of the sensors. To accomplish this, simulations were performed with the box standing still and rotating. The still simulation performed a perturbation on the sensors, showing the estimator accumulating the sensor values as they changed. The rotational simulation, while possibly unrealistic, involved the sensors being set to pre-defined values and having the box rotate based on a simulated step response. This perturbation demonstrated the ability of the estimator to track rotational positioning, necessary when estimating thermal distribution as the box rotates.



[Caption: A simulated run with the estimator, this graph shows the behavior of the estimator when provided with static sensor values as the box is rotated freely.]

## **Hardware**

Design decisions for the hardware were made upon customer requirements stating that the system must be able to operate on standby for up to two weeks and film at the end of that time. This required that the electronics draw very little power when not filming. To accomplish this end, the electronics were designed so as to allow the in-situ switching of power to various subsystems, such as the thermopile amplifiers and the motor driver circuitry.

# Power/Motor Driving Subsystem

#### Power Supply

Since the infrared camera requires 7.2V, the power supply of the housing robotics was tailored to accommodate that. To simplify this subsystem and remove as many failure modes as possible, Mikron was contacted to determine if a 7.4V supply was permissible. Upon their affirmative, the decision was made to use a 2-cell 7.4V Lithium Polymer (lipoly) battery to directly power the camera as opposed to using a switching supply from a 12V battery. When a fire is detected, the microcontroller asserts a signal to a MOSFET that connects the li-poly battery to the camera's power port.

The power conditioning for the microcontroller is planned as a simple and inexpensive linear regulator, while the final design may use a second, lower voltage battery to minimize quiescent current and improve efficiency. Since the processor only draws 2mA or so in active mode and less than 1mA in sleep mode [Atmel], an improved efficiency may not be necessary with the current battery configuration.

Since the system must be able to wait for as long as a couple weeks before the fire, reducing the power drawn during that time is critical. Along those lines, the fire sensing circuitry is planned to be powered down, when not in use, by disconnecting it from the battery supply. Every minute or so, the sensors will be activated briefly to check for fire and will again be turned off to conserve battery. Since the sensors themselves are unpowered, the start-up transient for the sensor system will be just from the amplifier circuitry and, while needing to be tested, is not expected to cause significant problems.

#### Motor Driver

The DC motor is powered by an H-Bridge switched by the PWM output on the microcontroller. While snubbing is not needed with the current motor/switching frequency configuration, the final build may require such circuitry.

#### Motor

The motor for controlling the position of the camera housing was chosen largely upon availability and its integrated quadrature encoder. When acquired, the motor was smaller than expected. Although it is anticipated to perform well enough for controller prototyping purposes, a larger motor might need to be acquired for the final box design.

## Optics Development and Selection

In order for the camera to observe the wildfire, a viewing port was needed to breach the insulation. To prevent the massive heat transfer inherent to an open viewport in combustion level conditions, a window was also needed.



Caption: The Mikron 7604 is capable of measuring heat using the 3.9µm wavelength. [Mikron]

In addition to blocking convective heat, the following requirements needed to be considered in order to not inhibit the thermal camera.

#### Window Selection Requirements:

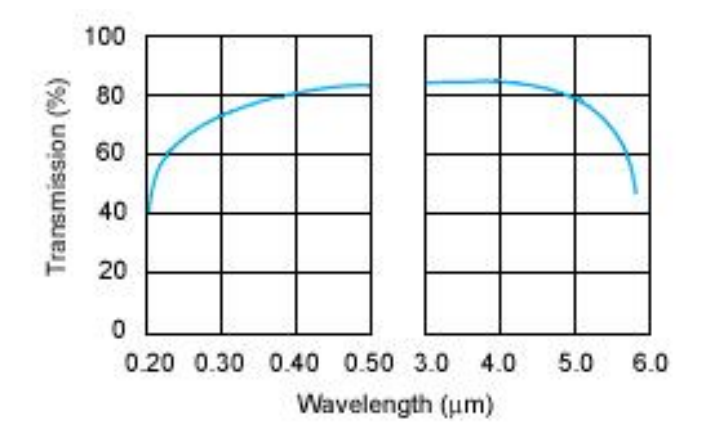
- Must be transmissive for 3.9μm infrared radiation, in order for the camera to function.
- Heat resilience: must be able to repeatably withstand direct contact with flame (1500°C)

Since silica-based glass is only transparent to visible light, custom optics were required to accomplish these requirements.

Material	Bandwidth	Melting Temperature
CaF <sub>2</sub>	0.17 – 7.80μm	Low
Al <sub>2</sub> O <sub>3</sub>	0.18 – 4.5μm	2030 °C
MgF <sub>2</sub>	0.12 – 8.50μm	1255 °C
Ge	2.0 – 14.0μm	Very Low
ZnSe	0.6 – 20 μm	1525 °C

Caption: List of known window materials [RedOptronics, Paper on CaF2 for IR, List of IR Window Materials]

The material chosen was  $Al_2O_3$ , also known as Sapphire. With its very high melting temperature and suitable pass-band, it was precisely what was needed. Additionally, being extremely hard, a Sapphire lens was better suited for the chaotic environment of a wildfire than the competing, softer window materials. The lens needed is currently being manufactured at RedOptronics, a custom optics supplier.



Caption: IR Sapphire window response curve.

## **Electronics**

The circuit design for the tracking and power management system was designed with power management in mind. In order to limit power consumption as much as possible, the ability to dynamically switch various subsystems on and off was implemented. Since the peripheral devices, such as the instrumentation amplifiers and motor driving circuitry draw a total quiescent current of 7mA, they were powered directly off the microcontroller

without external switching circuitry. While this reduced the part count, upon further analysis of the circuit following demoing, it was realized that the power draw of the H-Bridge may have exceeded the 20mA GPIO maximum of the Atmega168P. This would have dropped the rail on the instrumentation amplifiers also, creating the signal errors observed during the demonstration.

Depending on the operating voltage and clock speed, the Atmega168 is capable of drawing as low as .2 mA in active mode (1.8V, 1 MHz)[Atmel]. With the remainder of the subsystems disabled electronically, this translates to about 3.08 years of battery life on a 5.4 amp-hour battery as what is planned for use to power the camera. While actual power consumption would likely be larger than this, such a small power footprint could increase by almost two orders of magnitude before impinging on the two week battery life requirement. Since the majority of the power is to be reserved for the 5 Watt camera, this is desirable.

## **Software Designs**

The decision to use the Arduino framework was a decision driven by a well supported hardware and software knowledge base as well as extensive experience on John Thomson's part. As per standard practice, the program involved an initialization subroutine and an execution loop. Within the initialization routine, the values of the thermopiles were zeroed by averaging their starting voltages and using that as the baseline for all new measurements. This was needed due to thermal drift in the sensors.

Within the execution loop, several operations are executed periodically. First, the controller function is executed. For closed-loop position control, a controller was implemented with Proportional, Integral and Derivative feedback support. For the purpose of minimizing oscillations during testing, a P-D controller was used.

Next, the execution loop performs the "estimation" task, which implements the Bayesian filter described above[Fox]. The implementation of this algorithm weighted the probability distribution towards the front sensor, with the intention of creating a bias towards the front, subsequently requiring a large offset heat source to rotate the enclosure. The motivation for this was to prevent the box from flip-flopping between flickering heat sources. Belatedly, it was observed that this method was incorrect. Future work would involve normalizing the sensor estimations into a less weighted distribution and then performing the front bias logic externally to the estimator.

## **Future Work**

During final integration, many unforeseen problems became evident, many of which were unsolvable in the time remaining. While the use of a DC motor with an integrated encoder was convenient for developing closed loop control, it also presented significant complications. Since the motor was driven using a PWM signal, switching transients

created significant interference with other parts of the circuit.

Despite extensive attempts to reduce switching noise through bypass capacitors, snubbers and flyback diodes, the sensor amplifiers and the encoder both suffered from noise. It was determined that the integrated encoder was producing glitchy signals internally as a result of its proximity to the coils of the motor. Since these signals were being produced internally to the encoder, the signal produced could not easily be discerned as noise or useful signal through either software or hardware filtering. This presented the error of massive encoder slews whenever angular rotation was small and the motor PWM signal was being driven. Solutions to this issue would be to either replace the motor with a servo, a stepper motor, or separate the encoder from the motor.

Additionally, future work would include the integration of the system with the infrared camera. This is ideally done by simply switching its power on and using firmware to automatically begin recording. This feature would need to be developed in conjunction with the camera provider Mirkon.

In order to improve the stability and coherence of the electronics package, it would be desirable to create a PCB. While iteration constraints dictated the use of a perfboard, future iterations would see the circuit design stable enough to create a PCB that would dramatically improve space efficiency as well as help protect against circuit instabilities. Along with the PCB, additional improvements would include a clock reference to allow for faster debug output as well as external switching MOSFETs to power the peripherals instead of the microcontroller's GPIO.

## **Conclusion**

Two of the major components of global warming are the greenhouse gases emitted and environmental effects from wildfires. Tropical developing countries such as Brazil, Mexico and parts of Africa are of particular interest due to their diverse ecosystems and inhabitants that depend on fire for their sustainability. Solutions to this growing problem require the incorporation of modern science and technology to develop novel methods and tools to improve reduction strategies of environmental effects. Scientists currently utilize infrared imagery in laboratory settings to study and model wildfires through the combustion process—heating biomass, ignition of gases to produce flames and the transition from active flaming to smoldering and cooling. We planed to add to this body of research by developing an autonomous event driven fully rotational infrared camera built to withstand the heat of wildfires, orient itself toward an incoming wildfire and collect combustion level infrared imagery for modeling. The project is still underdevelopment the current status is that a prototype was developed to test the control system, rotational system and electrical system. Furthermore, thermal modeling and finding the parts required to complete the project have been decided upon. The current control system does not work fully as it has problems with fire tracking. However, the areas of failure have been identified and will be addressed in future iterations of the thermal camera.

## **References**

**Refractory Fixing** 

http://www.ancon.co.uk/downloads/s1/l1/refractory fixings october 2007 hr web .pdf

Mikron Infrared

http://www.mikroninfrared.com

RedOptronics, Sapphire specifications

http://www.redoptronics.com/sapphire-optical-material.html

Atmel, Product specifications for Atmega328

http://www.atmel.com/dyn/products/product\_card.asp?PN=ATmega328P

Paper on CaF2 for IR

http://jjap.ipap.jp/link?JJAP/20/L326/

List of IR Window Materials

http://www.atlas-inspection.com/infrared/irwindows.htm

Arduino Framework:

http://arduino.cc

Fox, Dieter. Position Estimation for Mobile Robots in Dynamic Environments

AAAI-98 and IAA-98 Proceedings